

Pions at finite temperature

Chungsik Song*

School of Physics and Astronomy, University of Minnesota, Minneapolis, Minnesota 55455

(Received 29 July 1993)

The properties of pions in hot hadronic matter are analyzed with an effective chiral Lagrangian which includes vector and axial-vector mesons. To obtain the dispersion relation and the absorptive properties of the pions in hot matter, the real and imaginary parts of the pion self-energy are calculated to one-loop order. The dispersion relation is very similar to that of free pions even at $T \sim 160$ MeV. The mean free path is estimated from the imaginary part of the self-energy. The mass is obtained from the pole position of the propagator and from the screening limit of the pion self-energy. Even though the deviation of the mass at finite temperature is small, both masses decrease as T increases. Pions remain massless in the chiral limit at finite temperature. Possible mixing of the pions with the A_1 mesons at finite temperature is discussed.

PACS number(s): 12.38.Mh, 12.40.Vv, 14.40.Aq

I. INTRODUCTION

A very hot and baryon-free region may be generated in high energy nucleus-nucleus collisions. If the energy density in the hot matter is high enough to exceed a critical value (~ 1 GeV/fm³), a new phase of QCD matter, the quark-gluon plasma, might be formed. As the system expands and cools down a phase transition and/or crossover to a hadron gas, which includes highly excited hadrons and resonances just after the transition, is expected. As the expansion and cooling continues these excited states decay, leading to a final state consisting mainly of pions. At presently available energies, central collisions generate final states containing several hundred pions. Actually, about 400 (300) pions are observed in O + Au (S + S) central collisions at 200 GeV/nucleon [1]. Because of the formation of the quark-gluon plasma and the expected phase transition, hadronic matter at finite temperature has been of great interest. In particular, the properties of pions in hot matter have been extensively studied [2-9].

At low temperature ($T < 100$ MeV), the hadronic matter mainly consists of pions which can be analyzed systematically in the framework of chiral perturbation theory at finite temperature [2-5]. The low energy theorems, which are obtained from current algebra and PCAC (partial conservation of axial-vector current), can be translated into a corresponding set of exact statements concerning the coefficients of the low temperature expansion. At finite temperature T , the typical pion energies are of order $E \sim T$. The interactions among the pions generate power corrections, controlled by the expansion parameter $T^2/8f_\pi^2$, where $f_\pi = 93$ MeV is the pion decay constant. At low temperature the pion interaction can be, therefore, treated as a perturbation.

However, the mean energy of pions in a heat bath of $T \approx 100$ MeV is of the order of 300 MeV, which is already too high for a systematic expansion in powers of temperature and energy to be useful. Moreover, in this range of temperature the pion properties are significantly affected by contributions from resonances, especially ρ mesons. To study pions at temperatures greater than 100 MeV we need to include the resonances explicitly and use an approach which does not rely on the low temperature expansion. It has been suggested that the expansion in powers of density is a reasonable approximation because hadronic matter is rather dilute even at $T \sim 150$ MeV [6]. The dispersive and absorptive properties of pions in hot matter are evaluated in the first order of the density, using experimental data for the $\pi\pi$ scattering amplitudes [7,8]. Recently this work has been extended to the second order in the density [9].

In this paper we use an effective chiral Lagrangian, which includes vector and axial-vector mesons explicitly, to describe the interaction of the pions in hot matter. The conventional finite temperature field theory is directly applied to the calculation of the pion properties at finite temperature. The modification of the pions in hot matter is included in the self-energy. The real and imaginary parts of the pion self-energy are evaluated from one-loop diagrams. We exploit the fact that the effective Lagrangian reproduces the experimental results at the tree level very well and the hadronic matter is rather dilute at $T < 150$ MeV.

In Sec. II, the pion self-energy at finite temperature is calculated with one-loop diagrams. There are six diagrams to be considered. Only for the dominant contributions are the detailed calculations and results shown. We have applied the same procedure to the other diagrams but the resulting expressions are too complicated to be written explicitly. In Sec. III, the dispersive and absorptive properties of the pions in hot hadronic matter are obtained from the real and imaginary parts of the pion self-energy calculated in Sec. II. The mean free path of the pion in hot matter can be evaluated from the imag-

*Present address: Cyclotron Institute, Texas A&M University, College Station, TX 77843.

inary part of the self-energy. In Sec. IV, we calculate the pion mass at finite temperature. Because there is no unique way to define the mass at finite temperature, we use two well-known definitions in many-body theory. We make some concluding remarks in Sec. V.

II. PION SELF-ENERGY

To describe hadronic matter at $T > 100$ MeV, we include the vector and axial-vector mesons as well as pions. We consider ρ , ω , and A_1 mesons which can be regarded

$$\mathcal{L} = \frac{1}{8}F_\pi^2 \text{Tr} D_\mu U D^\mu U^\dagger + \frac{1}{8}F_\pi^2 \text{Tr} M(U + U^\dagger - 2) - \frac{1}{2} \text{Tr}(F_{\mu\nu}^L F^{L\mu\nu} + F_{\mu\nu}^R F^{R\mu\nu}) + m_0^2 \text{Tr}(A_\mu^L A^{L\mu} + A_\mu^R A^{R\mu}) - i\xi \text{Tr}(D_\mu U D_\nu U^\dagger F^{L\mu\nu} + D_\mu U^\dagger D_\nu U F^{R\mu\nu}) + \sigma \text{Tr} F_{\mu\nu}^L U F^{R\mu\nu} U^\dagger, \quad (2.3)$$

where

$$U = \exp \left[\frac{2i}{F_\pi} \sum_i \frac{\phi_i \lambda_i}{\sqrt{2}} \right] \equiv \exp \left[\frac{2i}{F_\pi} \phi \right],$$

$$F_{\mu\nu}^{L,R} = \partial_\mu A_\nu^{L,R} - \partial_\nu A_\mu^{L,R} - ig[A_\mu^{L,R}, A_\nu^{L,R}], \quad (2.4)$$

$$D_\mu U = \partial_\mu U - ig A_\mu^L U + ig U A_\mu^R.$$

Note that D_μ is the chiral covariant derivative and g is the effective gauge coupling constant that should be determined phenomenologically. The degenerate spin-1 mass m_0 breaks gauge invariance but not chiral invariance, and the splitting of the degenerate mass occurs due to the partial Higgs mechanism. We include the mass term ($\sim M$) of Goldstone bosons which breaks chiral symmetry explicitly. The λ 's are the Gell-Mann matrices for $N_f = 3$ and Pauli matrices for $N_f = 2$. [In this section SU(3) notation is used.] We also include nonminimal coupling terms which are necessary to reproduce the experimental results. The ξ and σ are parameters that should be determined phenomenologically.

The anomalous interaction of the vector mesons are included explicitly in the effective Lagrangian through the gauged Wess-Zumino term which is given by [11]

$$\mathcal{L}_{\text{WZ}} = \frac{-gN_c}{48\pi^2} \epsilon^{\mu\nu\alpha\beta} \omega_\mu \text{Tr}[L_\nu L_\alpha L_\beta] + \frac{ig^2 N_c}{16\pi^2} \epsilon^{\mu\nu\alpha\beta} \omega_\mu \partial_\nu \text{Tr}[A_{R\alpha} L_\beta - A_{L\alpha} R_\beta] + ig(A_{R\alpha} U^\dagger A_{L\beta} U - A_{R\alpha} A_{L\beta}), \quad (2.5)$$

where N_c is the number of colors, $\epsilon^{\mu\nu\alpha\beta}$ is the antisymmetric Levi-Civita tensor with $\epsilon^{0123} = 1$, and L_α and R_α are the left and right Sugawara currents:

$$L_\alpha = U^\dagger \partial_\alpha U, \quad R_\alpha = U \partial_\alpha U^\dagger. \quad (2.6)$$

The pion self-energy at finite temperature is calculated based on this effective chiral Lagrangian with one-loop diagrams. In the effective Lagrangian approach at zero temperature, it is assumed that the properties of the system are describable at the tree level, where the masses and coupling constants are to be regarded as the physical ones. Loop diagrams, which are neglected, produce only renormalization effects on these parameters. There are

as gauge bosons of the $SU(2)_L \times SU(2)_R \times U(1)_V$ symmetry. The left-handed A_L^μ and right handed A_R^μ vector fields are related to the physical fields as

$$A_L^\mu = \frac{1}{2}(\rho^\mu + \omega^\mu + A_1^\mu), \quad (2.1)$$

$$A_R^\mu = \frac{1}{2}(\rho^\mu + \omega^\mu - A_1^\mu), \quad (2.2)$$

with $\rho^\mu = \rho_a^\mu \tau^a / \sqrt{2}$, $\omega^\mu = \omega^\mu \mathbf{1}$, $A_1^\mu = A_{1a}^\mu \tau^a / \sqrt{2}$, and τ_a 's are the Pauli matrices. The Lagrangian consists of nonlinear σ terms with covariant derivatives and Yang-Mills fields with mass terms [10]:

higher loop corrections and these loop corrections are already included effectively [12]. In finite temperature field theory there are corrections due to the interaction with the heat bath as well as the vacuum corrections. We use the fact that hadronic matter is rather dilute at the temperatures in which we are interested; for example, the mean free path of the pion is about 2 fm at $T \sim 150$ MeV. In this approximation the leading contribution to the temperature-dependent loop corrections is given by the process of a single interaction with a particle in the heat bath [13]. The one-loop approximation in finite temperature field theory includes both contributions from the tree diagrams at zero temperature and from the single interaction in the heat bath.

There are six diagrams which are to be considered (Fig. 1). The dominant contributions come from first two diagrams; other diagrams are suppressed by the Boltzmann factor since these diagrams have only heavy mesons as internal lines. We will consider only the first two diagrams. Mathematically these two diagrams are

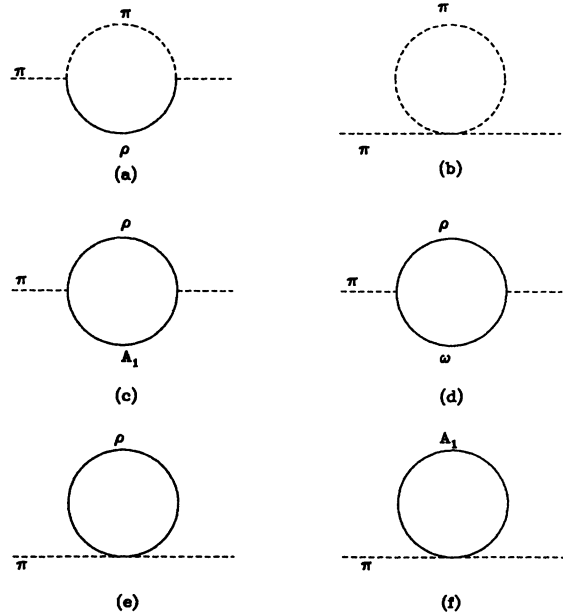


FIG. 1. One-loop diagrams for the pion self-energy.

$$\begin{aligned}
\Pi_{\pi}^{(a)} &= -ig^2 \int \frac{d^4 p}{(2\pi)^4} \int \frac{d^4 q}{(2\pi)^4} \left[(p_{\mu} - k_{\mu}) - \frac{\delta}{m_{\rho}^2} (k \cdot qp_{\mu} - p \cdot qk_{\mu}) \right] \frac{i}{p^2 - m_{\pi}^2} \\
&\quad \times \frac{i}{q^2 - m_{\rho}^2} \left(-g^{\mu\nu} + \frac{q^{\mu}q^{\nu}}{m_{\rho}^2} \right) \left[(p_{\nu} - k_{\nu}) - \frac{\delta}{m_{\rho}^2} (k \cdot qp_{\nu} - p \cdot qk_{\nu}) \right] (2\pi)^4 \delta^{(4)}(q - p - k), \\
\Pi_{\pi}^{(b)} &= -2g^2 \int \frac{d^4 p}{(2\pi)^4} \frac{i}{p^2 - m_{\pi}^2} \{5B_1 - 2B_2(k^2 + p^2) - 4B_3\tau[k^2 p^2 - (k \cdot p)^2]\}, \tag{2.7}
\end{aligned}$$

where [14]

$$\begin{aligned}
\delta &= 1 - \frac{(1 - \sigma)m_{\rho}^2}{(1 + \sigma)m_{A_1}^2} - \frac{2\xi g}{\sqrt{1 - \sigma}} \left(\frac{1 - \sigma}{1 + \sigma} \right) \frac{m_{\rho}^4}{m_{A_1}^4} \left(1 - \frac{(1 - \sigma)m_{\rho}^2}{(1 + \sigma)m_{A_1}^2} \right)^{-1}, \\
B_1 &= \frac{m_{\pi}^2}{6g^2 F_{\pi}^2}, \\
B_2 &= \frac{1}{g^2 F_{\pi}^2} \left(\frac{1}{3} - \frac{(1 - \sigma)m_{\rho}^2}{(1 + \sigma)m_{A_1}^2} \right), \\
B_3 &= \frac{g^4 F_{\pi}^4}{128m_{\rho}^8} - \frac{g\xi}{2\sqrt{1 - \sigma}} \frac{1}{m_{\rho}^4} \left(1 - \frac{(1 - \sigma)m_{\rho}^2}{(1 + \sigma)m_{A_1}^2} \right)^2. \tag{2.8}
\end{aligned}$$

In order to calculate the self-energy at finite temperature, we will replace the time component of momentum by i times the Matsubara frequency [15]. We make the replacement

$$p_0 \rightarrow 2n_p \pi T i, \quad q_0 \rightarrow 2n_q \pi T i, \quad k_0 \rightarrow 2n_k \pi T i, \tag{2.9}$$

and consequently integrals are replaced by a sum over modes,

$$\int \frac{dp_0}{2\pi} \rightarrow iT \sum_{n_p}, \quad \int \frac{dq_0}{2\pi} \rightarrow iT \sum_{n_q}, \tag{2.10}$$

where n is the integer.

Applying (2.9) and (2.10) to (2.7) gives

$$\begin{aligned}
\Pi_{\pi}^{(a)} &= ig^2 iT \sum_{n_p} iT \sum_{n_q} \int \frac{d^3 p}{(2\pi)^3} \int \frac{d^3 q}{(2\pi)^3} (2\pi)^3 \delta^3(\mathbf{q} - \mathbf{p} - \mathbf{k}) \frac{1}{iT} \delta_{n_q, n_p + n_k} \\
&\quad \times \left\{ (p - k)^2 + \frac{1}{m_{\rho}^2} [(p - k) \cdot q]^2 + \frac{2\delta}{m_{\rho}^2} \left[(k \cdot q)[p \cdot (p - k)] - (p \cdot q)[k \cdot (p - k)] \right] \right. \\
&\quad \left. + \frac{\delta^2}{m_{\rho}^4} \left[(k \cdot q)^2 p^2 + (p \cdot q)^2 k^2 - 2(p \cdot q)(k \cdot q)(p \cdot k) \right] \right\} \\
&\quad \times \frac{1}{[(2\pi T n_p)^2 + \omega_{\pi}^2(p)][(2\pi T n_q)^2 + \omega_{\rho}^2(q)]}, \\
\Pi_{\pi}^{(b)} &= -2g^2 T \sum_{n_p} \int \frac{d^3 p}{(2\pi)^3} \frac{5B_1 + 2B_2(k^2 + p^2) - 4B_3[k^2 p^2 - (k \cdot p)^2]}{(2\pi T n_p)^2 + \omega_{\pi}^2(p)}, \tag{2.11}
\end{aligned}$$

where we define

$$\omega_{\alpha}^2(p) = \mathbf{p}^2 + m_{\alpha}^2; \quad p^2 = (2\pi T n_p)^2 + \mathbf{p}^2. \tag{2.12}$$

The Matsubara summation can be done straightforwardly and the results are

$$\begin{aligned} \Pi_{\pi}^{(a)} = g^2 \int \frac{d^3 p}{(2\pi)^3} & \left\{ \frac{n(\omega_{\pi})}{2\omega_{\pi}} \left[\frac{H_0^+ - 2H_1^+ \mathbf{p} \cdot \mathbf{k} + H_2^+ (\mathbf{p} \cdot \mathbf{k})^2 - 2H_3 (\mathbf{p} \cdot \mathbf{k})^3}{R_{\pi}^+} \right. \right. \\ & \left. \left. + \frac{H_0^- - 2H_1^- \mathbf{p} \cdot \mathbf{k} + H_2^- (\mathbf{p} \cdot \mathbf{k})^2 - 2H_3 (\mathbf{p} \cdot \mathbf{k})^3}{R_{\pi}^-} \right] \right. \\ & \left. + \frac{n(\omega_{\rho})}{2\omega_{\rho}} \left[\frac{G[(p^2 k_0^2 + m_{\rho}^2 k^2) + 2\omega_{\rho} k_0 \mathbf{p} \cdot \mathbf{k} + (\mathbf{p} \cdot \mathbf{k})^2]}{R_{\rho}^+} \right. \right. \\ & \left. \left. + \frac{G[(p^2 k_0^2 + m_{\rho}^2 k^2) - 2\omega_{\rho} k_0 \mathbf{p} \cdot \mathbf{k} + (\mathbf{p} \cdot \mathbf{k})^2]}{R_{\rho}^-} \right] \right\}, \\ \Pi_{\pi}^{(b)} = -4g^2 \int \frac{d^3 p}{(2\pi)^3} & \frac{n(\omega_{\pi})}{2\omega_{\pi}} \left[5B_1 - 2B_2(k_0^2 - k^2 + m_{\pi}^2) + 4B_3[\mathbf{p}^2 k_0^2 + m_{\pi}^2 \mathbf{k}^2 + (\mathbf{k} \cdot \mathbf{p})^2] \right], \end{aligned} \quad (2.13)$$

where

$$\begin{aligned} R_{\pi}^{\pm} &= k_0^2 - k^2 - m_{\rho}^2 + m_{\pi}^2 \pm 2k_0 \omega_{\pi} - 2\mathbf{p} \cdot \mathbf{k}, \\ R_{\rho}^{\pm} &= k_0^2 - k^2 + m_{\rho}^2 - m_{\pi}^2 \pm 2k_0 \omega_{\rho} + 2\mathbf{p} \cdot \mathbf{k}, \end{aligned} \quad (2.14)$$

and

$$\begin{aligned} H_0^{\pm} &= -(k_0^2 - k^2 + m_{\pi}^2) + \frac{1}{m_{\rho}^2} (k_0^2 - k^2 - m_{\pi}^2)^2 \\ &\quad - \frac{\delta}{m_{\rho}^2} (p^2 k_0^2 + m_{\pi}^2 k^2) \\ &\quad \times \left[4 - \frac{\delta}{m_{\rho}^2} (k_0^2 - k^2 + m_{\pi}^2) \right] \\ &\quad \pm 2\omega_{\pi} k_0 \left[1 + \frac{\delta^2}{m_{\rho}^4} (p^2 k_0^2 + m_{\pi}^2 k^2) \right], \\ H_1^{\pm} &= 1 + \frac{\delta^2}{m_{\rho}^4} (p^2 k_0^2 + m_{\pi}^2 k^2 + 2\omega_{\pi}^2 k_0^2) \\ &\quad \mp \frac{\delta}{m_{\rho}^2} \omega_{\pi} k_0 \left[4 - \frac{\delta}{m_{\rho}^2} (k_0^2 - k^2 + m_{\pi}^2) \right], \\ H_2^{\pm} &= \frac{\delta}{m_{\rho}^2} \left[-4 + \frac{\delta}{m_{\rho}^2} (k_0^2 - k^2 + m_{\pi}^2) \right] \\ &\quad \pm \left(\frac{\delta}{m_{\rho}^2} \right)^2 6\omega_{\pi} k_0, \\ H_3 &= \frac{\delta^2}{m_{\rho}^4}, \\ G &= \frac{1}{m_{\rho}^2} (4 - 4\delta + \delta^2). \end{aligned} \quad (2.15)$$

There are temperature-independent terms (Π_{π}^{vac}) which are divergent. These are absorbed in the definition of the pion mass at zero temperature.

Integrating the vector over all angles can be done by writing

$$\mathbf{p} \cdot \mathbf{k} = pky, \quad y = \cos \theta, \quad (2.16)$$

where θ is the angle between \mathbf{p} and \mathbf{k} and $p \equiv |\mathbf{p}|$, $k \equiv |\mathbf{k}|$. Now the momentum integration becomes

$$\int \frac{d^3 p}{(2\pi)^3} = \frac{1}{(2\pi)^2} \int_0^{\infty} dp p^2 \int_{-1}^{+1} dy. \quad (2.17)$$

It is convenient to introduce the functions

$$\begin{aligned} P_n^{\pm} &= \int_{-1}^1 dy \frac{(pky)^n}{(k_0^2 - k^2 + m^2) \pm 2\omega k_0 + 2pky}, \\ Q_n^{\pm} &= \int_{-1}^1 dy \frac{(pky)^n}{(k_0^2 - k^2 + m^2) \pm 2\omega k_0 - 2pky}, \\ &= (-1)^n P_n^{\pm}, \end{aligned} \quad (2.18)$$

and

$$\Lambda_n^{\pm} \equiv P_n^+ \pm P_n^- = (-1)^n (Q_n^+ \pm Q_n^-). \quad (2.19)$$

With these definitions one may write

$$\begin{aligned} \Pi_{\pi} &= \Pi_{\pi}^{(a)} + \Pi_{\pi}^{(b)} \\ &= \frac{g^2}{4\pi^2} \int dpp^2 \left[\frac{n(\omega_{\pi})}{\omega_{\pi}} (-4B + \Lambda_{\pi 0} + 2\Lambda_{\pi 1} + \Lambda_{\pi 2} + 2\Lambda_{\pi 3}) \right. \\ &\quad \left. + \frac{n(\omega_{\rho})}{\omega_{\rho}} G[(p^2 k_0^2 + m_{\rho}^2 k^2) \Lambda_{\rho 0}^+ + 2\omega_{\rho} k_0 \Lambda_{\rho 1}^- + \Lambda_{\rho 2}^+] \right], \end{aligned} \quad (2.20)$$

where

$$\begin{aligned} \Lambda_{\pi i} &= \frac{1}{2} (H_i^+ + H_i^-) \Lambda_{\pi i}^+ + \frac{1}{2} (H_i^+ - H_i^-) \Lambda_{\pi i}^-, \\ \Lambda_{\pi i}^{\pm} &= \Lambda_i^{\pm}(\omega = \omega_{\pi}, m^2 = m_{\pi}^2 - m_{\rho}^2), \\ \Lambda_{\rho i}^{\pm} &= \Lambda_i^{\pm}(\omega = \omega_{\rho}, m^2 = m_{\rho}^2 - m_{\pi}^2), \end{aligned} \quad (2.21)$$

and

$$\begin{aligned} B &= 5B_1 - 2B_2(k_0^2 - k^2 + m_{\pi}^2) \\ &\quad + 4B_3(p^2 k_0^2 + m_{\pi}^2 k^2 + \frac{1}{3} k^2 p^2). \end{aligned} \quad (2.22)$$

To take care of the singularities in the definition of Λ_n^{\pm} , one has to add a small imaginary part to k_0 . We analytically continue k_0 from its Mastubara value to $k_0 = \omega - i\gamma$ where ω and γ are real. Then ω is the real frequency in

the dispersion relation and γ is the damping rate. We assume that $\gamma \ll \omega$; otherwise the oscillations do not propagate. This assumption will be checked later.

III. PROPAGATION OF PIONS

We consider the propagation of pions through a region containing matter in thermal equilibrium at temperature T . We find the dispersion relation by locating the poles of the propagator

$$\frac{1}{k_0^2 - k^2 - m_\pi^2 - \Pi(k_0, k)}. \quad (3.1)$$

This means we set

$$k_0^2 - k^2 - m_\pi^2 - \Pi(k_0, k) = 0. \quad (3.2)$$

The self-energy Π includes the physical condition prevailing in the medium which the pion traverses. If the medium is in thermal equilibrium, then Π is determined by the temperature. As mentioned in the previous section, the self-energy contains a singular integration, which indicates the self-energy has both real and imaginary parts. The imaginary part of Π determines the absorptive properties in hot matter while the dispersion relation depends on the real part. We may consider real wave numbers and identify the damping rate γ in terms of the imaginary part of the pole position in the k_0 plane,

$$k_0 = \omega - i\gamma. \quad (3.3)$$

To find the dispersion relation with a damping factor γ , we let $k_0 \rightarrow \omega - i\gamma$, and then solve for $\omega(k)$ and $\gamma(k)$:

$$\begin{aligned} 0 &= k_0^2 - k^2 - m_\pi^2 - \Pi(k_0, k) \\ &= (\omega - i\gamma)^2 - k^2 - m_\pi^2 - \Pi(\omega - i\gamma, k) \\ &= \omega^2 - k^2 - m_\pi^2 - \text{Re}[\Pi(\omega, k)] - \gamma \frac{\partial \text{Im}[\Pi(\omega, k)]}{\partial \omega} - i \left(\text{Im}[\Pi(\omega, k)] + 2\omega\gamma - \gamma \frac{\partial \text{Re}[\Pi(\omega, k)]}{\partial \omega} \right) + \dots \end{aligned} \quad (3.4)$$

The dispersion relation and the decay rate can be determined by the equations

$$\omega^2 - k^2 - m_\pi^2 - \text{Re}[\Pi(\omega, k)] \approx 0, \quad (3.5)$$

$$\text{Im}[\Pi(\omega, k)] + 2\omega\gamma \approx 0. \quad (3.6)$$

These relations are correct when the imaginary part of the self-energy is small, which should be examined first.

To calculate the imaginary part of the self-energy we apply the relation

$$\frac{1}{x - x_0 \pm i\epsilon} = \mathcal{P} \left[\frac{1}{x - x_0} \right] \mp i\pi\delta(x - x_0), \quad (3.7)$$

where \mathcal{P} is the principle value. There is no imaginary part in the tadpole diagram. The contribution from Fig. 1(a) is

$$\begin{aligned} \text{Im}[\Pi_\pi(\omega, k)] &= -\frac{g^2}{4\pi^2} \int p^2 dp \left\{ \frac{n(\omega_\pi)}{2\omega_\pi} \left[-\frac{[2(\omega^2 - k^2) - m_\rho^2 + 2m_\pi^2]}{2pk} + \frac{1}{m_\rho^2} \frac{(\omega^2 - k^2 - m_\pi^2)^2}{2pk} \right. \right. \\ &\quad \left. \left. + \frac{\delta}{m_\rho^2} (4 - \delta) \frac{4m_\pi^2(\omega^2 - k^2) - (\omega^2 - k^2 - m_\rho^2 + m_\pi^2)^2}{8pk} \right] \Theta_1 \right. \\ &\quad \left. - \frac{n(\omega_\rho)}{2\omega_\rho} \frac{1}{m_\rho^2} (4 - 4\delta + \delta^2) \left[\frac{4m_\rho^2(\omega^2 - k^2) - (\omega^2 - k^2 + m_\rho^2 - m_\pi^2)^2}{8pk} \right] \Theta_2 \right\}, \end{aligned} \quad (3.8)$$

where

$$\Theta_1 = \begin{cases} 1 & \text{if } ||A_1| - A_2| < p < |A_1| + A_2, \\ 0 & \text{otherwise,} \end{cases} \quad \Theta_2 = \begin{cases} 1 & \text{if } ||B_1| - B_2| < p < |B_1| + B_2, \\ 0 & \text{otherwise.} \end{cases}$$

A 's and B 's are given by

$$\begin{aligned} A_1 &= \frac{k(\omega^2 - k^2 - m_\rho^2 + m_\pi^2)}{2(\omega^2 - k^2)}, \\ A_2 &= \frac{|\omega|(\omega^2 - k^2 - m_\rho^2 + m_\pi^2)}{2|\omega^2 - k^2|} \sqrt{1 - \frac{4m_\pi^2(\omega^2 - k^2)}{(\omega^2 - k^2 - m_\rho^2 + m_\pi^2)^2}}, \\ B_1 &= \frac{k(\omega^2 - k^2 + m_\rho^2 - m_\pi^2)}{2(\omega^2 - k^2)}, \\ B_2 &= \frac{|\omega|(\omega^2 - k^2 + m_\rho^2 - m_\pi^2)}{2|\omega^2 - k^2|} \sqrt{1 - \frac{4m_\rho^2(\omega^2 - k^2)}{(\omega^2 - k^2 + m_\rho^2 - m_\pi^2)^2}}. \end{aligned} \quad (3.9)$$

The results are shown in Fig. 2. We find that the imaginary part rapidly increases with temperature and cannot be neglected when the temperature is greater than 160 MeV and the momentum is high ($k > 400$ MeV/c). The approximation we use breaks down at high temperature and high momentum where pions cannot propagate.

We calculate the mean free path λ which is defined by

$$\lambda = -\frac{k}{\text{Im}[\Pi(\omega, k)]} \quad (3.10)$$

as a function of the momentum. We find a very strong momentum dependence of the mean free path (Fig. 3). The mean free path tends to zero as $k \rightarrow 0$ because the collision time for a massive particle at rest is finite. λ reaches a maximum at about $k \approx 50$ MeV, the position of the maximum being approximately independent of T .

We carefully apply Eq. (3.5) for the dispersion relation at low temperature and low momentum. The evaluation of the real part of the self-energy can be easily done when we use the relations

$$\begin{aligned} \text{Re}[\Lambda_{\alpha 0}^+] &= \frac{1}{2pk} L_{\alpha}^+, \\ \text{Re}[\Lambda_{\alpha 0}^-] &= \frac{1}{2pk} L_{\alpha}^-, \\ \text{Re}[\Lambda_{\alpha 1}^+] &= 2 - \frac{k_0^2 - k^2 + m^2}{4pk} L_{\alpha}^+ - \frac{k_0 \omega_{\alpha}}{2pk} L_{\alpha}^-, \\ \text{Re}[\Lambda_{\alpha 1}^-] &= -\frac{k_0 \omega_{\alpha}}{2pk} L_{\alpha}^+ - \frac{k_0^2 - k^2 + m^2}{4pk} L_{\alpha}^-, \\ \text{Re}[\Lambda_{\alpha 2}^+] &= -(k_0^2 - k^2 + m^2) + \frac{(k_0^2 - k^2 + m^2)^2 + 4\omega_{\alpha}^2 k_0^2}{8pk} L_{\alpha}^+ + \frac{k_0 \omega_{\alpha} (k_0^2 - k^2 + m^2)}{2pk} L_{\alpha}^-, \\ \text{Re}[\Lambda_{\alpha 2}^-] &= -2k_0 \omega_{\alpha} - \frac{k_0 \omega_{\alpha} (k_0^2 - k^2 + m^2)}{2pk} L_{\alpha}^+ - \frac{(k_0^2 - k^2 + m^2)^2 + 4\omega_{\alpha}^2 k_0^2}{8pk} L_{\alpha}^-, \\ \text{Re}[\Lambda_{\alpha 3}^+] &= \frac{2}{3} p^2 k^2 + \frac{1}{2} [(k_0^2 - k^2 + m^2)^2 + 4\omega_{\alpha}^2 k_0^2] - \frac{(k_0^2 - k^2 + m^2)^3 + 12k_0^2 \omega_{\alpha}^2 (k_0^2 - k^2 + m^2)}{16pk} L_{\alpha}^+ \\ &\quad - \frac{6k_0 \omega_{\alpha} (k_0^2 - k^2 + m^2)^2 + 8k_0^3 \omega_{\alpha}^3}{16pk} L_{\alpha}^-, \end{aligned} \quad (3.11)$$

where

$$\begin{aligned} L_{\alpha}^+ &= \ln \left| \frac{(k_0^2 - k^2 + m^2 + 2pk)^2 - 4\omega_{\alpha}^2 k_0^2}{(k_0^2 - k^2 + m^2 - 2pk)^2 - 4\omega_{\alpha}^2 k_0^2} \right|, \\ L_{\alpha}^- &= \ln \left| \frac{(k_0^2 - k^2 + m^2)^2 - 4(\omega_{\alpha} k_0 + pk)^2}{(k_0^2 - k^2 + m^2)^2 - 4(\omega_{\alpha} k_0 - pk)^2} \right|. \end{aligned} \quad (3.12)$$

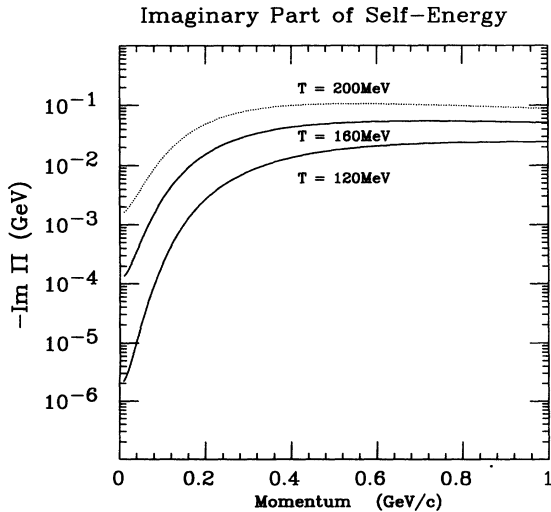


FIG. 2. Imaginary part of the self-energy at $T=120, 160,$ and 200 MeV.

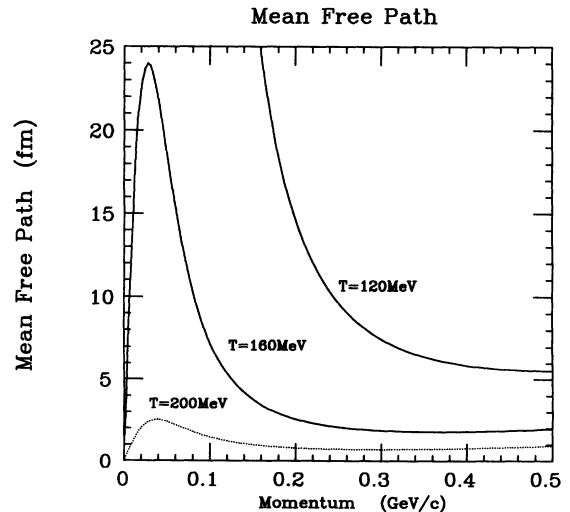


FIG. 3. Mean free path of the pion at $T=120, 160,$ and 200 MeV.

We find

$$\begin{aligned}
\text{Re}[\Pi_\pi(\omega, k)] = & \frac{g^2}{4\pi^2} \int p^2 dp \left\{ \frac{n(\omega_\pi)}{2\omega_\pi} \left[4 - 8B + \left(\frac{\delta}{m_\rho^2} \right) (4 - \delta)(\omega^2 - k^2 - m_\rho^2 + m_\pi^2) \right. \right. \\
& + 4 \left(\frac{\delta}{m_\rho^2} \right)^2 m_\pi^2 k^2 + 4 \left(\frac{\delta}{m_\rho^2} \right)^2 \left(\frac{1}{3} k^2 + \omega^2 \right) p^2 \\
& \left. \left. - \frac{2(\omega^2 - k^2) - m_\rho^2 + 2m_\pi^2 - \frac{1}{m_\rho^2}(\omega^2 - k^2 - m_\pi^2)^2}{2pk} L_\pi \right. \right. \\
& \left. \left. + \left(\frac{4\delta - \delta^2}{m_\rho^2} \right) \frac{[4m_\pi^2(\omega^2 - k^2) - (\omega^2 - k^2 - m_\rho^2 + m_\pi^2)^2]}{8pk} L_\pi \right] \right. \\
& \left. - \frac{n(\omega_\rho)}{2\omega_\rho} \left(\frac{4 - 4\delta + \delta^2}{m_\rho^2} \right) \left[(\omega^2 - k^2 + m_\rho^2 - m_\pi^2) \right. \right. \\
& \left. \left. + \frac{4m_\rho^2(\omega^2 - k^2) - (\omega^2 - k^2 + m_\rho^2 - m_\pi^2)^2}{8pk} L_\rho \right] \right\}, \quad (3.13)
\end{aligned}$$

where

$$\begin{aligned}
L_\pi &= L_\pi^+(m^2 = m_\pi^2 - m_\rho^2), \\
L_\rho &= L_\rho^+(m^2 = m_\rho^2 - m_\pi^2). \quad (3.14)
\end{aligned}$$

Now Eq. (3.5) can be solved numerically in a self-consistent way. The results are shown in Fig. 4 at $T=120$ and 160 MeV. The dotted line is the results obtained when we include all diagrams. We can see that the other four diagrams are negligible as expected. The dispersion relations are very close to free particles except near $k \approx 400$ MeV/ c where the imaginary part gets large and our assumption breaks down. The results are very similar to those obtained by using the experimentally measured scattering amplitude [7,8].

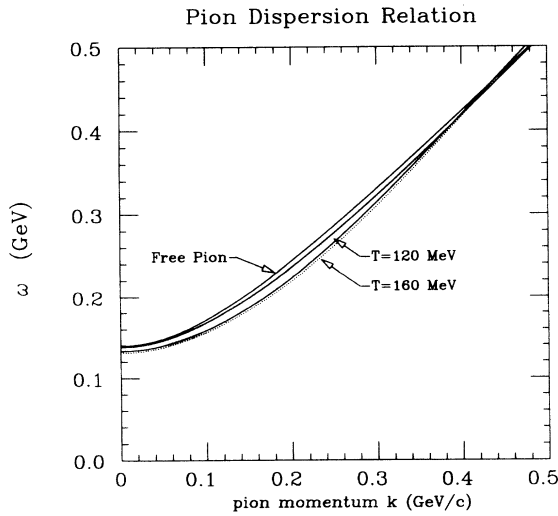


FIG. 4. Dispersion relation of the pion in hot matter at $T=120$ and 160 MeV. The dotted line is obtained when we include all diagrams shown in Fig. 1.

IV. MASS OF PIONS

Hadron masses at finite temperature have been extensively examined recently because the symmetry property of the hadronic system might be reflected in the mass of the hadrons [16]. Since the masses of the low-lying hadrons are strongly correlated with the quark condensate, which is responsible for the spontaneous breaking of the chiral symmetry, hadron masses are expected to change as the symmetry gets restored. The mass of the pion has been of interest because the pion plays a special role as the Goldstone boson of the broken symmetry and so its properties are very sensitive to the symmetry of

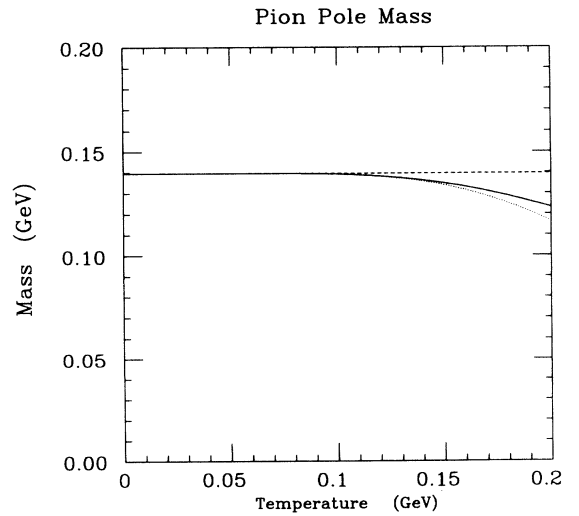


FIG. 5. Effective mass determined from the pole position of the propagator. The dotted line is the total contribution from all diagrams and the solid line is the contribution from the two diagrams considered in the text. The dashed line is the result in the chiral limit.

the system. The change of the pion mass at finite temperature is expected to be weak, since the Gell-Mann–Oakes–Renner relation might hold at finite temperature [17]:

$$m_\pi(T) \sim \sqrt{-m_q \langle \bar{q}q \rangle_T / f_\pi^2(T)}, \quad (4.1)$$

where the mass is determined from the pole of the propagator, $D_\pi(\omega, \mathbf{q})$, in the limit $\mathbf{q} \rightarrow 0$. This shows that, because of the small quark mass m_q , the tempera-

ture dependence of $m_\pi(T)$ is expected to be weaker than that of other hadrons.

The mass of the particle is not uniquely defined at finite temperature because of the lack of the Lorentz invariance of the system. There are several definitions which are used in different contexts. One may define the effective pion mass as the pole position of the propagator. This pole mass can be obtained from the Eq. (3.2) in the limit $\mathbf{k} \rightarrow 0$:

$$\omega^2 - m_\pi^2 - \text{Re}[\Pi_\pi(\omega, \mathbf{k} \rightarrow 0)] = 0. \quad (4.2)$$

In the limit $\mathbf{k} \rightarrow 0$,

$$L_\alpha^+ \rightarrow \frac{k_0^2 + m^2}{\Delta_\alpha} 8pk + \left(-\frac{1}{\Delta_\alpha} + \frac{2(k_0^2 + m^2)(k_0^2 + m^2 - 2p^2)}{\Delta_\alpha^2} + \frac{16p^2(k_0^2 + m^2)}{3\Delta_\alpha^3} \right) 8pk^3 + O(k^5), \quad (4.3)$$

where

$$\Delta_\alpha = (k_0^2 + m^2)^2 - 4\omega_\alpha^2 k_0^2. \quad (4.4)$$

Substituting these expressions to Eq. (3.13) yields

$$\begin{aligned} \text{Re}[\Pi_\pi(\omega, \mathbf{k} \rightarrow 0)] = & \frac{g^2}{4\pi^2} \int dp p^2 \left\{ \frac{n(\omega_\pi)}{2\omega_\pi} \left[Q_1 + Q_2 p^2 + Q_3 \frac{\omega^2 - m_\rho^2 + m_\pi^2}{(\omega^2 - m_\rho^2 + m_\pi^2)^2 - 4\omega_\pi^2 \omega^2} \right] \right. \\ & \left. + \frac{n(\omega_\rho)}{2\omega_\rho} \left(\frac{4 - 4\delta + \delta^2}{m_\rho^2} \right) \frac{4p^2 \omega^2 (\omega^2 + m_\rho^2 - m_\pi^2)}{(\omega^2 + m_\rho^2 - m_\pi^2)^2 - 4\omega_\rho^2 \omega^2} \right\}, \end{aligned} \quad (4.5)$$

where

$$\begin{aligned} Q_1 &= 4 + \frac{\delta}{m_\rho^2} (4 - \delta) (\omega^2 - m_\rho^2 + m_\pi^2) - 8[5B_1 - 2B_2(\omega^2 + m_\pi^2)], \\ Q_2 &= 4\omega^2 \left[\left(\frac{\delta}{m_\rho^2} \right)^2 - 8B_3 \right], \\ Q_3 &= -4(2\omega^2 - m_\rho^2 + 2m_\pi^2) + \frac{4}{m_\rho^2} (\omega^2 - m_\pi^2)^2 + \frac{\delta}{m_\rho^2} (4 - \delta) [4\omega^2 m_\pi^2 - (\omega^2 - m_\rho^2 + m_\pi^2)^2]. \end{aligned} \quad (4.6)$$

Now Eq. (3.13) can be solved self-consistently. The pole mass is given in Fig. 5 as a function of temperature. As temperature increases the pole mass of the pion decreases, but the change is very small, as expected from the Gell-Mann–Oakes–Renner relations [$\Delta m_\pi(T) \sim 10$ MeV at $T = 160$ MeV]. This behavior is opposite to the result of chiral perturbation theory, which shows an increase of the pion mass with temperature [2]. However, one can find a similar decrease in the pion mass at finite temperature (up to 160 MeV) in the Nambu–Jona-Lasinio model [18] and linear σ model calculations [19]. We should note that there are uncertainties near the phase transition region ($T \sim 150$ MeV) for all of these approaches.

In lattice simulations the screening mass, which can be obtained from the static infrared limit of the self-energy, is widely used. The screening mass of pions can be written as

$$m_\pi^{sc} = \sqrt{m_\pi^2 + \text{Re}[\Pi_\pi(\omega = 0, \mathbf{k} \rightarrow 0)]}. \quad (4.7)$$

In the static infrared limit we have

$$L_\alpha^+ \rightarrow \frac{8pk}{m^2} + \frac{8pk^3}{m^4} + O(k^5). \quad (4.8)$$

The real part of the self-energy in the static infrared limit is

$$\text{Re}[\Pi_\pi(\omega = 0, \mathbf{k} \rightarrow 0)] = -\frac{4}{3} \frac{m_\pi^2}{F_\pi^2} \int \frac{p^2 dp}{(2\pi)^2} \frac{n(\omega_\pi)}{2\omega_\pi}. \quad (4.9)$$

The screening mass of the pion can be obtained from Eqs. (4.7) and (4.9), and is shown in Fig. 6. Even though there is a slight decrease, the screening mass is almost constant at temperatures we consider. When we compare the result with that obtained from the pole position, we get different values at $T > 100$ MeV (Fig. 7). This result reminds us to be careful of the definition of mass at finite temperature.

In the chiral limit where $m_\pi^{\text{vac}} = 0$, the effective Lagrangian has an explicit chiral $SU(N_f)_L \times SU(N_f)_R$ symmetry which is spontaneously broken in the hadron phase. The pions are regarded as the massless Goldstone bosons corresponding to the broken symmetry. This means that the pion should remain massless at low temperature as long as the chiral symmetry remains broken. We can see explicitly that the screening mass, defined from the static infrared limit of the real part for the self-energy, becomes zero in the chiral limit. One can show that the pole mass goes to zero as the mass of the pion becomes zero. This fact can be checked numerically. In Fig. 8 the dispersion relations of the pions in the chiral limit are shown. The pole mass can be read from the dispersion curve at the limit $\mathbf{k} \rightarrow 0$. These indicate the self-consistency of our Lagrangian and approximation to describe the broken symmetry phase.

V. CONCLUSION

We have analyzed the pion properties in hot hadronic matter. The analysis is based on the effective chiral Lagrangian with vector and axial-vector mesons. We assume rather low density of the hadronic matter at $T = 100\text{--}150$ MeV. We believe that the approximation is reasonable to describe the hadronic system up to the phase transition.

The self-energy of the pion is approximated by the one-loop diagrams. The imaginary part of the self-energy is

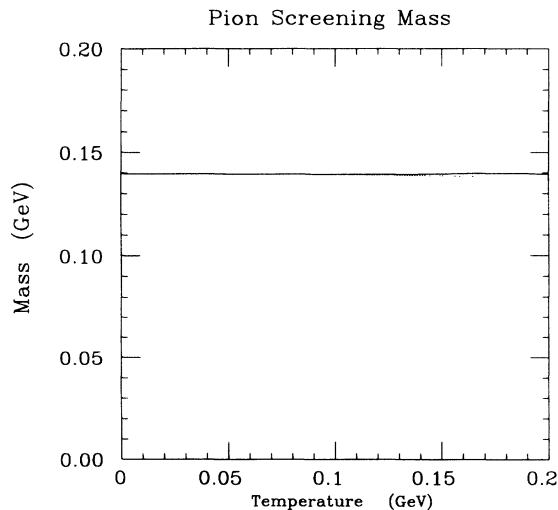


FIG. 6. Screening mass as a function of temperature. The dotted line is the total contribution from all diagrams and the solid line is the contribution from the two diagrams considered in the text.

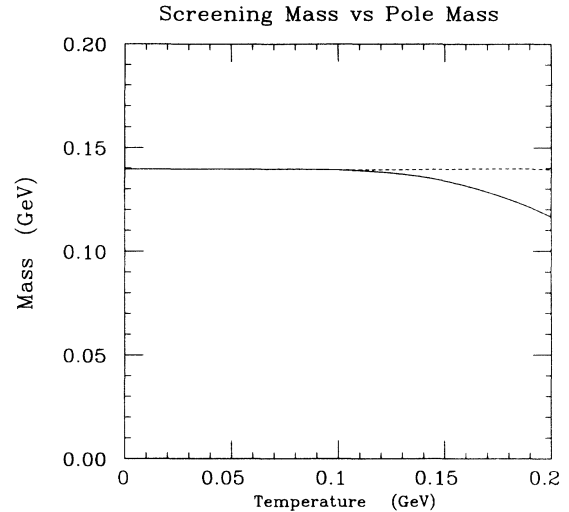


FIG. 7. Comparison between the screening mass (dashed line) and pole mass (solid line).

rather big when the temperature is bigger than 160 MeV and momentum is bigger than 400 MeV/ c . In this region we cannot analyze the pion propagation consistently and the pion might not propagate. The mean free path of the pion is very small in the high temperature and high momentum region. At low momentum there are peaks and the mean free path is bigger than the size of the hot system formed in a nucleus-nucleus collision (5–8 fm). One would expect that any particles with a mean free path greater than the size of the system could not be thermalized [2]. This suggests that low momentum pions may escape the hot zone without interaction and have a small chance to be thermalized.

The dispersion relation of the pion is obtained at low momentum with the assumption that the imaginary part of the self-energy is small. When the temperature is less than 160 MeV the dispersion relation is very similar to

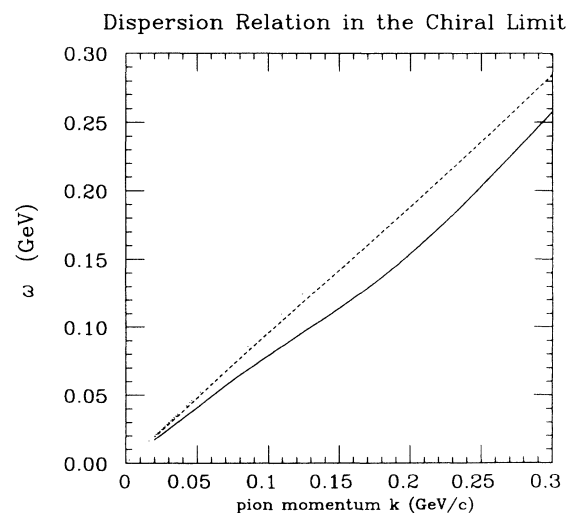


FIG. 8. Dispersion relation of the pion in the chiral limit when $T=120$ (dashed line) and 160 MeV (solid line). The dotted line is the result for free pion.

that of the free pion gas. Even though there is an increasing attractive force which pulls down the dispersion curve, the modification of the pion dispersion relation is not enough to produce a dip or flattening. When the momentum of the pion gets close to 400 MeV/c we can see that the group velocity of the pion is bigger than 1, which contradicts causality. However, such a behavior can be seen in electrodynamics when there is an anomalous absorption, and it is not in contradiction with causality. The large group velocity of the pions, similarly, indicates strong absorption of the pion in hot matter. In this range the damping is high and the propagating modes are absorbed after times which are very short so that the group velocity has no longer any meaning. This modification in the dispersion relation of the pion might be observed in the spectrum of dileptons from hot hadronic matter.

The mass of the pion is determined in two different ways and different values of the mass are obtained at finite temperature. This reflects the different physical properties of screening and of propagation. Both masses show a slight decrease with increasing T and become zero in the chiral limit.

There is an interesting possibility of a mixing of the pion and A_1 mesons at finite temperature. The diagram which is responsible for this mixing is shown in Fig. 9. The diagram represents the possible process in which the pion (A_1 meson), which passes through medium, inter-

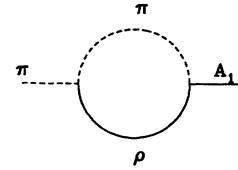


FIG. 9. Mixing of the pions with the A_1 mesons at finite temperature.

acts with a pion or a rho meson in the heat bath, and converts to the A_1 meson (pion). Because of the momentum dependence of the couplings, the contribution of this diagram to the self-energy can be written as i times an integral which includes a singularity. The detail calculation of the integral shows that the pion mass, which is obtained in the limit either $\mathbf{k} \rightarrow 0$ or $k_0 = 0$, $\mathbf{k} \rightarrow 0$, is not affected by the mixing. It is expected that its contribution to the real part of the self-energy is very small. However, it is interesting enough to deserve future investigation.

ACKNOWLEDGMENTS

I am very grateful to J. I. Kapusta for many useful discussions and a critical reading of the manuscript. This research was supported by the U.S. Department of Energy under Grant No. DOE/DE-FG02-87ER-40328.

-
- [1] A. Bamberger *et al.*, Phys. Lett. B **203**, 320 (1988); T. J. Humanic *et al.*, Z. Phys. C **38**, 79 (1988); H. Ströbele *et al.*, *ibid.* **38**, 89 (1988); W. J. Harris *et al.*, in *Quark Matter '88*, Proceedings of the Seventh International Conference on Ultrarelativistic Nucleus-Nucleus Collisions, Lenox, Massachusetts, 1988, edited by G. Baym, P. Braun-Munzinger, and S. Nagamiya [Nucl. Phys. **A498**, 133c (1989)]; R. Renfordt *et al.*, *ibid.* **A498**, p. 385c.
 - [2] J. Gasser and H. Leutwyler, Phys. Lett. B **188**, 477 (1987).
 - [3] P. Gerber and H. Leutwyler, Nucl. Phys. **B321**, 387 (1987).
 - [4] J. L. Goity and H. Leutwyler, Phys. Lett. B **184**, 83 (1989); **228**, 425 (1989).
 - [5] P. Gerber, H. Leutwyler, and J. Goity, Phys. Lett. B **246**, 513 (1990); H. Bebie, P. Gerber, J. L. Goity, and H. Leutwyler, Nucl. Phys. **B378**, 95 (1987).
 - [6] H. Leutwyler and A. V. Smilga, Nucl. Phys. **B342**, 302 (1990).
 - [7] E. V. Shuryak, Nucl. Phys. **A533**, 761 (1991).
 - [8] A. Schenk, Nucl. Phys. **B363**, 97 (1991).
 - [9] A. Schenk, Phys. Rev. D **47**, 5138 (1993).
 - [10] For details see Chungsik Song, Phys. Rev. D **48**, 1375 (1993), and references therein.
 - [11] U.-G. Meissner and I. Zahed, Z. Phys. A **327**, 5 (1987).
 - [12] B. W. Lee and H. T. Nieh, Phys. Rev. **166**, 1507 (1968).
 - [13] J. I. Kapusta, in *Trends in Theoretical Physics*, edited by P. Ellis and Y. C. Tang (Addison-Wesley, Redwood City, CA, 1991), Vol. 2; E. V. Shuryak, Nucl. Phys. **A533**, 761 (1991).
 - [14] The coupling constant g and the pion decay constant F_π are the physical values redefined after diagonalization. See [10].
 - [15] J. I. Kapusta, *Finite Temperature Field Theory* (Cambridge University Press, Cambridge, England, 1989).
 - [16] R. J. Furnstahl, T. Hatsuda, and Su H. Lee, Phys. Rev. D **42**, 1744 (1990); T. Hatsuda, Y. Koike, and Su H. Lee, *ibid.* **47**, 1225 (1992); Nucl. Phys. **B394**, 221 (1993).
 - [17] H. Hatsuda and T. Kunihiro, Prog. Theor. Phys. Suppl. **91**, 284 (1987).
 - [18] T. Kunihiro, Nucl. Phys. **B351**, 593 (1991).
 - [19] A. Gocksh, Phys. Rev. Lett. **67**, 1701 (1991).